applied sciences

MDPI

Article

Energy-Efficient User Pairing for Downlink NOMA in Massive MIMO Networks

Mahmoud Ahmed El-ghorab [1,2,*], Mohamed Rihan El-meligy [3], Mohamed Mostafa Ibrahim [4] and Fatma Newagy [1]

[1] Department of Electronics and Communications, Faculty of Engineering, Ain Shams University (ASU), Cairo 11566, Egypt; fatma_newagy@eng.asu.edu.eg
[2] Department of Communication and Computer Engineering, Higher Institute of Engineering, El-Shorouk City 11837, Egypt
[3] Department of Electronics and Communication Engineering, Faculty of Electronic Engineering, Menoufia University, Menouf City 32951, Egypt; mohamed.elmeligy@el-eng.menofia.edu.eg
[4] Department of Electrical Engineering, Faculty of Engineering, Suez Canal University, Ismailia 41522, Egypt; m.mostafa@eng.suez.edu.eg
* Correspondence: m.elghorab@sha.edu.eg

Abstract: The motivations for deploying energy and spectral-efficient network architectures are the high energy consumption and the need for more spectral resources in modern cellular networks. The key method to solve the energy efficiency (EE) maximization problem of the downlink non-orthogonal multiple access (NOMA)-based massive MIMO system is to decouple it into user pairing and efficient power allocation problems. This work studies the performance of three main pairing methods in NOMA-based networks: Hungarian, Gale–Shapley, and correlation-based approaches. Firstly, we provide a mathematical analysis for EE of downlink NOMA in a massive MIMO system for the non-line of sight (NLoS) channel model with perfect successive interference cancellation (SIC). Finally, the sequential convex programming (SCP) approach is used to tackle the power allocation problem. Simulation results show that the Hungarian algorithm for pairing plus SCP for power allocation (Hungarian algorithm-SCP) achieves the highest energy efficiency among all the three pairing algorithms with an identical performance to joint user and resource block association with power allocation (joint user-RB PA) algorithm but with much lower computational complexity and outperforms the NOMA SCP greedy algorithm (NOMA-SCP-GA).

Keywords: user pairing; NOMA; massive MIMO; Hungarian; Gale–Shapley; 5G

Citation: El-ghorab, M.A.; El-meligy, M.R.; Ibrahim, M.M.; Newagy, F. Energy-Efficient User Pairing for Downlink NOMA in Massive MIMO Networks. *Appl. Sci.* **2022**, *12*, 5421. https://doi.org/10.3390/app12115421

Academic Editor: Mario Marques Da Silva

Received: 12 April 2022
Accepted: 22 May 2022
Published: 27 May 2022

1. Introduction

The most important challenge for 5G networks is to face the huge increase in mobile data traffic. One of the promising technologies to improve spectral efficiency (SE) is the use of non-orthogonal multiple access (NOMA) [1,2]. NOMA techniques are able to support the incorporation of billions of Internet of Things (IOT) devices with a more efficient use of spectrum [3]. In power domain NOMA, users with poor channel gains are assigned more power than users with better channel gains [4]. Users with poor channels deal with interference as noise, whereas users with higher channels depend on SIC to eliminate the interference. One of the main challenges for applying SIC is the need to have perfect channel state information (CSI), which necessitates the use of downlink pilot signaling. Additionally, computational complexity is another obstacle in the execution of SIC [5]. Moreover, NOMA has multiple challenges, e.g., dynamic user pairing algorithms, receivers utilizing low complexity SIC, and optimal resource allocation schemes [6–11]. One of the crucial NOMA schemes is the sparse code multiple access (SCMA) scheme, where the bits are mapped to sparse codewords by the SCMA encoder after multi-dimensional modulation and low density spreading [12]. The major advantage of the SCMA scheme

is the provided shaping gain. Another important NOMA scheme is the non-orthogonal pattern division multiple access (PDMA) scheme proposed in [13]. Data symbols of users are guaranteed to be of adequate diversity disparity and power disparity by careful design of the patterns of different users. This improves the performance by allowing the use of low-complexity SIC-based multi-user detection. On a parallel theme, massive MIMO technology has been proposed to improve the SE of 5G communication networks [14] and enhance system capacity [15]. In massive MIMO, the base station (BS) communicates simultaneously with multiple mobile stations (MSs) on the same time–frequency resources. Massive MIMO systems can support hundreds or even thousands of antenna channels in the array [16]. The possibility of applying large antenna arrays faces many challenges, e.g., high complexity and power consumption [17,18]. The integration of massive MIMO and NOMA offers a great opportunity to improve the SE in 5G and beyond. EE is now an important demand in designing wireless communication networks. Typically, EE is defined as the number of reliably transmitted bits per one joule [19]. It shows the cost paid in power consumption to afford a certain throughput as a service quality metric. The considered energy efficiency optimization problem is a joint user pairing and power allocation problem. The problem is decoupled into two subproblems for less complexity. The user pairing subproblem is solved by applying three different pairing methods: Hungarian, Gale–Shapley, and correlation. The second sub-problem of power allocation is formulated as a fair energy efficiency maximization problem and solved by applying sequential convex optimization.

1.1. Background

An algorithm of low computational complexity is proposed in [20] to solve the user scheduling, link selection, and power allocation problems for D2D cellular networks with NOMA technology. The proposed algorithm achieves high data rates and converges in a limited number of iterations. NOMA and OMA are compared for a large number of BS antennas in [21]. Karush–Kuhn–Tucker (KKT) conditions are used to derive closed-form solution for maximizing the sum rate of downlink NOMA system [22]. Moreover, the pairing of two users of different channel conditions is accomplished using the Hungarian algorithm. The work in [23] studies the joint power allocation and user association for EE maximization in multi-cell multi-carrier NOMA (MCMC-NOMA) networks. A new binary variable matrix for the association is introduced in [24] to allow dynamic pairing for NOMA-assisted downlink networks. The work in [25] applies a clustering strategy of low complexity and introduces KKT optimality conditions to obtain a closed-form result of power allocation for EE maximization in downlink NOMA systems. The stochastic algorithm, two-stage greedy randomized adaptive search (GRASP), and two-stage stochastic sample greedy (SSD) are three heuristic solutions proposed in [26] to optimize the problem of efficient dynamic power and channel allocation (DPCA) for users in the downlink multi-channel NOMA (MC-NOMA) systems. An efficient joint multi-resource-block optimization scheme is proposed in [27] to achieve an optimal weighted achievable rate (WAR) for NOMA-based maritime communications. A NOMA-assisted ambient backscatter communication (AmBC) system is proposed in [28] to increase the achievable sum rate. The work in [29] decomposes the multi-dimensional resource allocation problem for MIMO-NOMA systems into beamforming, user clustering, and power allocation. At first, a fractional transmitting power control (FTPC) is applied. Then, optimal user clustering is considered. Finally, power allocation is introduced as a difference of convex (DC) programming problem to be solved by successive convex approximation (SCA). Hybrid spatial division multiple access (SDMA) and NOMA are combined in [30] for optimal power allocation in sectored cells for sum-throughput maximization. Integer linear programming is adopted in [31] for user pairing, and particle swarm optimization is used for power allocation in NOMA systems in 5G networks. The work in [32] classifies users according to their status into cell-center users, high-rate edge users, and low-rate edge users to participate in many-to-many subchannel–user matching problems to form joint transmission coordinated multi-point (JT-CoMP) subchannels and dynamic point selection CoMP (DPS-CoMP) subchannels. The work

in [33–36] introduced the power allocation solution for maximizing the EE in power domain NOMA. Dynamic power allocation and four different pairing methods for NOMA in heterogeneous networks were introduced in [37].

The EE maximization for an uplink NOMA-assisted mmWave mMIMO system was considered in [38], and a hybrid analog-digital beamforming scheme was proposed to reduce the number of radio frequency chains at the BS. In [39], EE maximization of an uplink hybrid system with NOMA integrated with OMA (HMA) was achieved, and a minimum required rate is pre-defined for each user to guarantee the quality of service. The problem is decoupled into the user-resource block association subproblem, and the power allocation subproblem and (joint user-RB PA) algorithm is proposed. User clustering, sub-channel allocation, and power allocation are jointly considered in the EE optimization problem for the uplink multi carrier-NOMA network in [40]. A user pairing algorithm that ensures the cluster fairness in terms of the sum rate gain is proposed in [41], and a comparison between MIMO-NOMA and MIMO-OMA when users have pre-defined quality of service (QoS) requirements is also conducted. In [42], EE is maximized through a user-pairing approach, utilizing the greedy algorithm and power allocation utilizing SCP. The NOMA-SCP-GA algorithm is proposed to solve the problem.

1.2. Contributions

In this work, we solve the EE maximization problem for the downlink NOMA-based massive MIMO system; for short, it is named the NOMA-based scheme, through decoupling into the user pairing subproblem and fair power allocation subproblem to reduce complexity. Firstly, we study the energy efficient user pairing for zero forcing (ZF) beamforming. Then, we mathematically formulate the max-min EE into a non-convex fractional programming problem, which is transformed into a sequence of subtractive form, followed by the SCP approach to obtain the optimal solution. Different from [22], we study the performance of a massive MIMO system and its effect on power consumption calculations and power allocation solution. Additionally, we consider the max-min utility function for EE in the power allocation solution. Additionally, Ref. [23] introduced a matching-based framework to accomplish user association and subcarriers' assignment. The Gale–Shapley algorithm used in our work is a matching-based framework and is outperformed by the Hungarian algorithm, as is obvious from the results. The work in [24] gave two solutions for the fairness rate maximization problem. The first is based on relaxation and inner approximation and does not guarantee a globally optimal solution, whereas the second solution uses the channel correlation as the weights of edges on the bipartite graph for user pairing. Both of them are of high computational complexity, which leads to high power consumption. The main contributions in this paper are listed as follows:

- We consider the evaluation of three different user-pairing approaches. Results are compared to obtain the optimal user pairing approach to maximize EE for downlink NOMA. We show how the pairing decisions affect the performance of the NOMA-based scheme.
- Propose a novel power allocation scheme based on the sequential convex programming (SCP) to iteratively update the power assignment vector that will eventually optimize EE.

For comparison, the proposed algorithms are compared with the joint user-RB PA algorithm and NOMA-SCP-GA in terms of SE and EE. The remaining part of this paper is described as follows: In Section 2, the system model is described. In Section 3, the power consumption model for the downlink NOMA-based scheme is introduced. In Section 4, the different pairing approaches are discussed. Section 5 presents the proposed power allocation scheme. In Section 6, the complexity analysis is introduced. The simulation results are discussed in Section 7. Finally, the paper is concluded in Section 8.

2. System Model

Consider a single-cell system, where the set of single-antenna users is represented as $\{1, \ldots, U\}$. Users are served by an A-antenna BS with $A \gg U$. The served users are divided into two equal groups, where the first group contains the cell-center users $u_c \in U_c$ and $U_c = \{1, \ldots, U/2\}$. The second group contains the cell-edge users $u_e \in U_e$ and $U_e = \{U/2 + 1, \ldots, U\}$.

The downlink channel vector for user u is described as

$$\mathbf{g}_u = \sqrt{\beta_u}\mathbf{h}_u \quad u = 1, \ldots, U. \tag{1}$$

where β_u is the large scale fading coefficient, which represents the path-loss factor only, and the effect of shadowing is neglected. The system is in the time division duplex (TDD) mode, which provides the advantage of channel reciprocity that permits using the uplink pilots in estimating the downlink channels. For the NLoS channels, we use coherence intervals, where the channels are constant and frequency flat. The channel of user u is $\mathbf{h}_u$, which follows independent Rayleigh fading distribution as the small scale fading realization $\mathbf{h}_u \sim CN(\mathbf{0}, \mathbf{I}_A)$, and $\mathbf{I}_A$ represents the identity matrix. The NOMA-based scheme system model is presented in Figure 1, where each NOMA group contains one cell-center user paired with a cell-edge user.

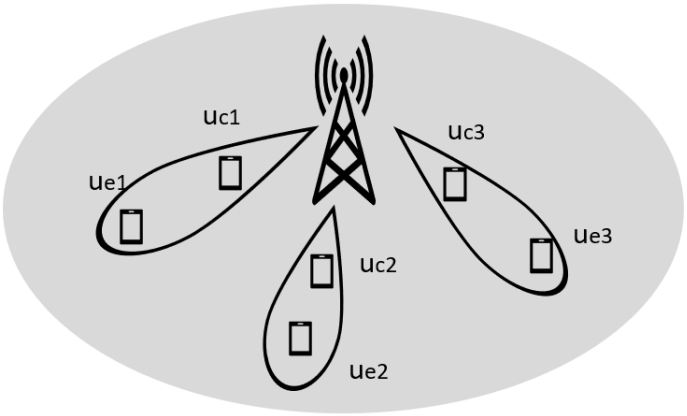

Figure 1. NOMA-based scheme network model.

3. Energy Efficiency

Considering the energy efficiency as the performance metric of interest, defined as the ratio between throughput in (bit/s/cell) and the total power consumption in (W/cell) as follows [19]:

$$\text{EE} = \frac{Throughput(\text{bit/s/cell})}{power\ consumption(\text{W/cell})} = \frac{R}{\gamma}. \tag{2}$$

The power consumption γ for a downlink NOMA-based scheme consists of the effective transmitted power $ETpower$ and the circuit power consumption $Cpower$. The $ETpower$ takes the efficiency of power amplifier ξ into consideration, such that

$$\gamma = ETpower + Cpower, \tag{3}$$

$$ETpower = \frac{1}{\xi}\sum_{u=1}^{U} q_u. \tag{4}$$

where q_u is the BS transmitted power to user u. The circuit power consumption $Cpower$ is the sum of different components according to [19]. Additionally, $Cpower$ represents the

power consumed by encoding and decoding $P_{cod/dec}$, power consumed by the signaling of backhaul P_{bh}, and power consumed by digital signal processing P_{sp}.

$$Cpower = P_{fix} + P_{tc} + P_{ce} + P_{cod/dec} + P_{bh} + P_{sp}. \quad (5)$$

where P_{fix} stands for the load independent power of infrastructure and power of control signaling, and P_{tc} represents the power consumed by transceiver chains, which is calculated according to the following equation:

$$P_{tc} = AP_{BS} + P_{lo} + UP_{UE}. \quad (6)$$

where P_{BS} is the power required to operate the circuit components of the BS, e.g., analog-to-digital converters, I/Q mixers, and modulators/demodulators. P_{lo} is the power consumed by the local oscillator. P_{UE} is the power consumed by circuit components in the user equipment. For the downlink, P_{cod} is the power in watt/bit/s required to encode throughput R in bit/s at BS, and P_{dec} is the power required to decode R at the user equipment.

$$P_{cod/dec} = (P_{cod} + P_{dec})R. \quad (7)$$

where P_{bh} is the power required by the load-dependent backhaul as follows:

$$P_{bh} = P_{bt}.R. \quad (8)$$

where P_{bt} is the power of the backhaul traffic in watt/bit/s. Additionally, P_{ce} stands for the power consumed in channel estimation:

$$P_{ce} = \frac{3B}{ML_{bs}}(U)\left(A\tau + A^2\right). \quad (9)$$

We have B/M coherence blocks/s, where B is the communication bandwidth and M is the number of samples per coherence block. L_{bs} is the computational efficiency of BS measured in flops/s. The power consumed by digital signal processing P_{sp} is computed as

$$P_{sp} = P_{sp-t} + P_{sp-c}^{DL} + P_{sp-pairing}^{DL}. \quad (10)$$

P_{sp-t} stands for the power consumed in the downlink transmission.

$$P_{sp-t} = \frac{3B}{ML_{bs}}AU\tau_d. \quad (11)$$

where $\tau_d = (1 - U/M)$ is the part used for downlink data in each coherence interval since uplink data are not considered here. P_{sp-c}^{DL} is the power required for computing the beamforming vector.

$$P_{sp-c}^{DL} = \frac{4B}{ML_{bs}}A\left(\frac{U}{2}\right). \quad (12)$$

For the NOMA-based scheme, only $\frac{U}{2}$ beamforming vectors are computed. The power consumed in applying the Gale–Shapley algorithm for pairing, which is executed every coherence block, which means $\frac{B}{M}$ times/s. The factor $\left(\frac{U}{2}\right)^2$ is according to the computational complexity calculations.

$$P_{sp-pairing}^{DL} = \frac{3B}{ML_{bs}}\left(\frac{U}{2}\right)^2. \quad (13)$$

4. Proposed User Pairing Solutions

Users are divided into two main groups. The first group represents cell-center users of high channel gains, and the second group represents cell-edge users of low channel gains.

The pairing algorithm selects one cell-center user with one cell-edge user to form a NOMA group that guarantees maximum EE in NOMA based scheme.

4.1. Gale–Shapley Algorithm

The user pairing problem is formulated as follows:

$$Maximize \sum_{u_c=1}^{U/2} \sum_{u_e=U/2+1}^{U} F_{u_c,u_e} \mathrm{EE}. \tag{14}$$

where

$$F_{u_c,u_e} = \begin{cases} 1 & ;\text{if the } u_c \text{ is already paired with } u_e \\ 0 & ;\text{if the } u_c \text{ is not paired with } u_e \end{cases}$$

The Gale–Shapley algorithm considers the stable marriage criteria to obtain pairs. Every user in the first group forms its own preference list of the other group members [37]. The preferences of each member of the first group are arranged in descending order to guarantee that they propose to the most preferred users of the second group. Members of the second group have the right to accept the proposal if they are free or decline if they prefer their current partners. Members of the second group have the right to choose between their current partners and the new proposals. For users of the first group who did not get partners in the first round of proposals, they propose again according to the sequence of their preference list. The values of the preference list are computed according to (14). The output of the pairing process is stable if there is no user from the first group and a user from the second group who are not paired to each other, but both prefer each other over their current partners. For the Gale–Shapley algorithm, the output is stable for the group that offers the proposals. The Gale–Shapley algorithm is presented in Algorithm 1. An example of the preference list for six users is introduced in Table 1.

Algorithm 1 The GS algorithm.

Step 1:
Each cell-center user forms a list of its preferences in cell-edge users in descending order according to EE calculations.
Step 2:
(a) Each unpaired cell-center user gives a pairing request to the cell-edge user he prefers most.
(b) Each cell-edge user replies "yes" to the cell-center user he most prefers and "no" to all other cell-center users. The cell-edge user is then provisionally "paired" to the cell-center user he most prefers so far, and that cell-center user is temporarily "paired" to that cell-edge user.
Step 3:
(a) Each unpaired cell-center user gives a pairing request to the most-preferred cell-edge user to whom he has not yet given a pairing request (regardless of whether that cell-edge user is already paired)
(b) Each cell-edge user replies "yes" if he is currently not paired or if he prefers this cell-center user over his current temporary partner (in this case, the cell-edge user rejects his current temporary partner who becomes unpaired).
Step 4:
This process is repeated until everyone is paired.

Table 1. The preference list of the cell-center users.

	First Group Preferences		
u_{c1}	u_{e1}	u_{e3}	u_{e2}
u_{c2}	u_{e3}	u_{e1}	u_{e2}
u_{c3}	u_{e1}	u_{e3}	u_{e2}

4.2. Hungarian Algorithm

The Hungarian algorithm is used for solving single agent to single task assignment problem [22]. It is initially designed to solve minimization problems, so we generate an objective optimization matrix of EE calculations between cell-center users and cell-edge users as shown in Table 2. The target now is to pick the pairs that maximize EE. To convert the optimization problem to a minimization problem, the optimization objective matrix is modified and converted to the cost matrix δ_{cost}. The modification process starts with finding the maximum of each column, then all column elements are subtracted from their corresponding maximum value as shown in Table 3. The resultant matrix is the cost matrix to be minimized. Minimization of the cost matrix is a maximization of the optimization objective matrix. The Hungarian algorithm is summarized in Algorithm 2. The optimization problem is now formulated as follows:

$$Minimize \sum_{u_c=1}^{U/2} \sum_{u_e=U/2+1}^{U} F_{u_c,u_e}\delta_{cost} \tag{15}$$

$$F_{u_c,u_e} = \begin{cases} 1 & ;\text{if the } u_c \text{ is already paired with } u_e \\ 0 & ;\text{if the } u_c \text{ is not paired with } u_e \end{cases}$$

Algorithm 2 The Hungarian algorithm.

Step 1: Create a cost matrix.
Step 2: Find the smallest element in each row and subtract it from every element of that row. Repeat this process for each column.
Step 3: Tag all zeros as starred or primed, where the starred zeros represent an independent set of zeros and primed zeros represent the possible candidates.
Step 4: Cover each column containing a starred zero. If $\frac{U}{2}$ columns are covered. Go to done, otherwise go to step 5.
Step 5: Prime an uncovered zero. If there is no starred zero in the row containing the primed zero, go to step 6. Otherwise, cover this row and uncover the column containing starred zero. Continue in this manner until there are no uncovered zeros left. Save the smallest uncovered value and go to step 7.
Step 6: Continue generating a series of alternating primed and starred zeros until this series ends at a primed zero that has no starred zero in its column. Unstar each starred zero, star each primed zero, erase all primes, and uncover every line. Return to step 4.
Step 7: Subtract the value found in step 5 from every element of each uncovered column and add it to every element of each covered row. Return to step 5 without altering any primes, stars, or covered lines.
Step 8: The position of starred zeros in the cost matrix indicates the paired users that maximize EE.

Table 2. An example of the optimization objective matrix for the Hungarian algorithm.

	u_{e1}	u_{e2}	u_{e3}
u_{c1}	8 G bit/joule	10 G bit/joule	14 G bit/joule
u_{c2}	8 G bit/joule	8 G bit/joule	16 G bit/joule
u_{c3}	12 G bit/joule	13 G bit/joule	4 G bit/joule

Table 3. The cost matrix δ_{cost} to be minimized.

	u_{e1}	u_{e2}	u_{e3}
u_{c1}	4	3	2
u_{c2}	4	5	0
u_{c3}	0	0	12

4.3. Correlation-Based Pairing

Here, the pairing is based on the similarities between channels of cell-center users and cell-edge users [21]. After the estimation of channel vectors, the BS forms NOMA groups based on correlation between the channels estimates. The high correlation value indicates that the beamforming vector will match both users in the NOMA pair. The correlation between the channel of cell-center user u_c and cell-edge user u_e is given as

$$\rho_{u_c,u_e} = \frac{|\hat{\boldsymbol{h}}_{u_c}\hat{\boldsymbol{h}}_{u_e}^{H}|}{\|\hat{\boldsymbol{h}}_{u_c}\|\|\hat{\boldsymbol{h}}_{u_e}\|}. \tag{16}$$

5. Power Allocation Solution

In this work, the fairness between cell-center users and cell-edge users is guaranteed by formulating the objective function as a max-min energy efficiency problem. This optimization problem is expressed mathematically as

$$\begin{aligned} \max_{\mathbf{q}\geq 0} \; & min \quad \text{EE} \\ \text{Subject to} \quad & C_1 : \sum_{u=1}^{U} q_u \leq q_{max} \\ & C_2 : R_u \geqslant R_{min} \qquad \forall u \in U_c \\ & C_3 : R_u \geqslant eR_{min} \qquad \forall u \in U_e. \end{aligned} \tag{17}$$

where R_{min} is the minimum data rate for cell-center users. The factor e is inserted to ensure that cell-edge users are targeting smaller rate eR_{min}, where $0 < e < 1$. The formulated problem is a fractional problem and it is transformed into a series of parametric subtractive-form subproblems as follows:

$$\begin{aligned} \max_{\mathbf{q}\geq 0} \; & min \quad R - \text{EE}\ \gamma \\ \text{Subject to} \quad & C_1, C_2, C_3. \end{aligned} \tag{18}$$

The objective function in (18) is a non-convex problem and it needs to be reformulated.

$$R - \text{EE}\gamma = X(\mathbf{q}) - Z(\mathbf{q}), \tag{19}$$

where,

$$\begin{aligned} X(\mathbf{q}) = B\, log_2 \Bigg[& \left(\beta_{u_c} \sum_{\substack{i\neq u_c \\ i\neq u_{ce}}}^{U} q_i |\mathbf{h}_{u_c}^T \mathbf{w}_i|^2 + q_{u_c}\beta_{u_c}|\mathbf{h}_{u_c}^T \mathbf{w}_{u_c}|^2 + 1 \right) \\ & \left(\beta_{u_e} \sum_{i\neq u_e}^{U} q_i |\mathbf{h}_{u_e}^T \mathbf{w}_i|^2 + q_{u_e}\beta_{u_e}|\mathbf{h}_{u_e}^T \mathbf{w}_{u_e}|^2 + 1 \right) \Bigg] - \text{EE}\gamma, \end{aligned} \tag{20}$$

$$Z(\mathbf{q}) = B\, log_2\left[\left(\beta_{u_c}\sum_{\substack{i\neq u_c\\ i\neq u_{ce}}}^{U} q_i|\mathbf{h}_{u_c}^T\mathbf{w}_i|^2+1\right)\left(\beta_{u_e}\sum_{i\neq u_e}^{U} q_i|\mathbf{h}_{u_e}^T\mathbf{w}_i|^2+1\right)\right]. \tag{21}$$

where $\mathbf{w}_u$ is the ZF beamforming vector for user u. The non-convex constraints C_2 and C_3 are reformulated into a convex form after some mathematical manipulations. The new constraints C_2^{new} and C_3^{new} are given by

$$C_2^{new}: q_{u_c}\beta_{u_c}|\mathbf{h}_{u_c}^T\mathbf{w}_{u_c}|^2+\left(1-2^{R^{min}/B}\right)\left(\beta_{u_c}\sum_{\substack{i\neq u_c\\ i\neq u_{ce}}}^{U} q_i|\mathbf{h}_{u_c}^T\mathbf{w}_i|^2+1\right)\geqslant 0. \tag{22}$$

$$C_3^{new}: q_{u_e}\beta_{u_e}|\mathbf{h}_{u_e}^T\mathbf{w}_{u_e}|^2+\left(1-2^{eR^{min}/B}\right)\left(\beta_{u_e}\sum_{i\neq u_e}^{U} q_i|\mathbf{h}_{u_e}^T\mathbf{w}_i|^2+1\right)\geqslant 0. \tag{23}$$

Reformulate (18) as

$$\begin{aligned}&\max_{\mathbf{q}\geq 0} min \quad X(\mathbf{q})-Z(\mathbf{q})\\ &\text{Subject to} \quad C_1, C_2^{new}, C_3^{new}.\end{aligned} \tag{24}$$

Both functions $X(\mathbf{q})$ and $Z(\mathbf{q})$ are concave. Thus, the objective $X(\mathbf{q})-Z(\mathbf{q})$ is a difference of two concave functions. Using the first-order Taylor expansion,

$$Z(\mathbf{q})\approx Z\left(\mathbf{q}^{(k-1)}\right)+\bigtriangledown Z^T\left(\mathbf{q}^{(k-1)}\right)\left(\mathbf{q}-\mathbf{q}^{(k-1)}\right). \tag{25}$$

where $\bigtriangledown Z(\mathbf{q})$ is the gradient of $Z(\mathbf{q})$ at $\mathbf{q}$ and is formulated in (26). $\mathbf{q}^k$ is obtained as an optimal solution at the k-th iteration. The vector gradient of Z at $\mathbf{q}$ is given by

$$\bigtriangledown Z(\mathbf{q}) = \frac{1}{\left(\beta_{u_c}\sum\limits_{\substack{i\neq u_c\\ i\neq u_{ce}}}^{U} q_i|\mathbf{h}_{u_c}^T\mathbf{w}_i|^2+1\right)}f_1+\frac{1}{\left(\beta_{u_e}\sum\limits_{i\neq u_e}^{U} q_i|\mathbf{h}_{u_e}^T\mathbf{w}_i|^2+1\right)}f_2, \tag{26}$$

where $f_1(u_c)$, $f_1(u_{ce})$, and $f_2(u_e)$ equal zero

$$f_1(i) = \frac{B\beta_{u_c}|\mathbf{h}_{u_c}^T\mathbf{w}_i|^2}{ln2} \quad i\neq u_c \text{ and } i\neq u_{ce}, \tag{27}$$

$$f_2(i) = \frac{B\beta_{u_e}|\mathbf{h}_{u_e}^T\mathbf{w}_i|^2}{ln2} \quad i\neq u_e. \tag{28}$$

A new variable $\eth$ is introduced to smooth the optimization function. Then, we formulate the $\eth$ optimization problem for the NOMA-based scheme as follows:

$$\begin{aligned}&\underset{\mathbf{q}\geq 0}{maximize} \quad \eth\\ &\text{Subject to} \quad C_1, C_2^{new}, C_3^{new}\\ &\qquad\qquad C_4: X(\mathbf{q})-Z\left(\mathbf{q}^{(k-1)}\right)-\bigtriangledown Z^T\left(\mathbf{q}^{(k-1)}\right)\left(\mathbf{q}-\mathbf{q}^{(k-1)}\right)\geqslant \eth.\end{aligned} \tag{29}$$

The final objective function in (29) can be effectively solved to obtain the objective sub-optimal power allocation solution. To obtain the optimal $\eth_{optimum}$ that gives the optimal power allocation, we apply the bisection-based iterative algorithm shown in Algorithm 3, where the search domain is halved in each iteration to guarantee fast convergence.

Algorithm 3 Bisection algorithm for solving the max-min fairness power allocation problem.

1: **Input**: q_{max}, tolerance $\epsilon > 0$
2: **output**: q_u for u = 1,...,U.
3: **Initialization**: set $\eth^{lower} = 0$ and $\eth^{upper} = min\left(\frac{R}{\gamma}\right)$.
4: **Calculate**: $\eth = \frac{\eth^{upper} + \eth^{lower}}{2}$.
5: **Solve**: (29) using the sequential convex approximation for $\eth$ and evaluate q_u.
6: If feasible: then $\eth^{lower} \leftarrow \eth$ and $q_u = q_{optimum}$ for u = 1,...,U.
7: Else $\eth^{upper} \leftarrow \eth$
8: **while**: $\eth^{upper} - \eth^{lower} > \epsilon$

The procedures of finding the iterative power allocation using convex software packages for a given $\eth$ is given in Algorithm 4.

Algorithm 4 Iterative SCP power allocation for obtaining q.

1: **Initialize**: $k = 0$ and $\mathbf{q}^{(0)}$
2: **Repeat**:
3: **Solve**: the feasibility problem in (29)
Subject to $C_1, C_2^{new}, C_3^{new}, C_4$
4: **Set**: $k = k + 1$.
5: **Until**: $\mathbf{q}^{(k)}$ converges.

6. Complexity Analysis

By considering that the number of users in the scenario is U, the computational complexity of the Gale–Shapley algorithm depends on the number of iterations until convergence. It is computed as $O\left(\left(\frac{U}{2}\right)^2\right)$. The complexity of the Hungarian algorithm is calculated as the number of iterations needed to find the optimal pairs, which is $O\left(\left(\frac{U}{2}\right)^3\right)$. The complexity of correlation calculations for the NLoS scenario is $O\left(U^2 A\right)$ since the numerator requires (A) complex multiplications and the denominator has neglected computational complexity for norm calculations and single values multiplication. The process is repeated (U^2) times. The power solution is solved based on the SCP approach, using Algorithm 2, which converges in (J_2) iterations. The transformation process performed in Algorithm 1, namely the bisection method, requires (J_1) iterations. Since our model contains (U) users, the computational complexity of power solution using algorithm-1 and algorithm-2 is $O\left(J_1 J_2 U\right)$. Hence, the computational complexity of our solution is

$$Complexity\ of(correlation - SCP) = O\left(U^2 A + J_1 J_2 U\right) \tag{30}$$

$$Complexity\ of(GSalgorithm - SCP) = O\left(\left(\frac{U}{2}\right)^2 + J_1 J_2 U\right) \tag{31}$$

$$Complexity\ of(Hungarianalgorithm - SCP) = O\left(\left(\frac{U}{2}\right)^3 + J_1 J_2 U\right) \tag{32}$$

compared to the computational complexity of NOMA-SCP-GA after applying in our problem

$$Complexity\ of(NOMA - SCP - GA) = O\left(\left(\frac{U}{2}\right)^2 + J_3 J_4 U\right) \tag{33}$$

where J_3 *and* J_4 are numbers of iterations till convergence according to [42]. The computational complexity of joint user-RB PA utilized to solve our problem in our network model is given as

$$Complexity\ of(Joint\ user-RB\ PA) = O\left(\left(\frac{U}{2}\right)^3 + J_5 J_6 J_7 U^2\right) \quad (34)$$

where J_5, J_6, *and* J_7 are numbers of iterations till convergence according to [39].

7. Results

Performance Evaluation

In our simulation, the importance of having a correlation between channels must be considered in channel generation. The high correlation helps eliminate interference from other pairs, which improves the weak user's rate. Thus, the correlation between users' channels helps weak users in different pairs have an obvious impact on the system performance metric and highlights the effect of the user pairing process. The simulation parameters applied are introduced in Table 4.

Table 4. Simulation parameters.

Parameter	Value
Path and penetration loss at distance d (km)	130 + 37.6 $log_{10}(d)$.
Cell edge length	350 m
Coherence interval length (in symbols)	100
Fixed power: P_{fix}	5 W
Power of BS lo: P_{lo}	0.1 W
Power per BS antennas: P_{BS}	0.2 W
Power per UE: P_{UE}	0.1 W
Power for data encoding: P_{cod}	0.01 W/(Gbit/s)
Power for data decoding: P_{dec}	0.08 W/(Gbit/s)
BS computational efficiency: L_{bs}	750 Gflops/W
Power for backhaul traffic: P_{bt}	0.025 W/(Gbit/s)

Figure 2 represents EE for the mMIMO-based scheme presented in [21], compared to EE for NOMA-based scheme with fixed pairing, where users of each pair are specified. Results show that the mMIMO-based scheme achieves higher EE for a lower number of users, where the $A >> U$ condition is satisfied. The superiority of mMIMO decreases as U increases till reaching $U = 21$, where the NOMA-based scheme starts to lead. $A >> U$ is the condition for a system to be considered a massive MIMO system. When this condition is not satisfied with the increasing number of users, the effect of integration of NOMA with massive MIMO on EE improvement is vital.

Figure 3 shows EE in bit/joule for different user numbers at a fixed number of BS antennas $A = 36$. The EE increases with increasing U. Results show that correlation-SCP, Hungarian algorithm-SCP, and joint user-RB PA achieve the same EE performance, even with different values of U. They outperform the GSalgorithm-SCP and NOMA-SCP-GA by about 5 M bit/joule with $U = 24$.

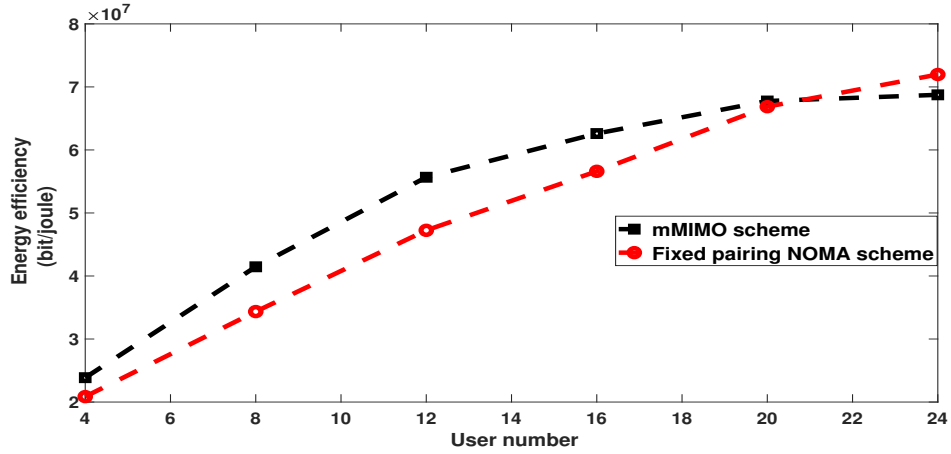

Figure 2. EE for mMIMO-based scheme versus NOMA-based scheme, with $A = 36$ BS antennas.

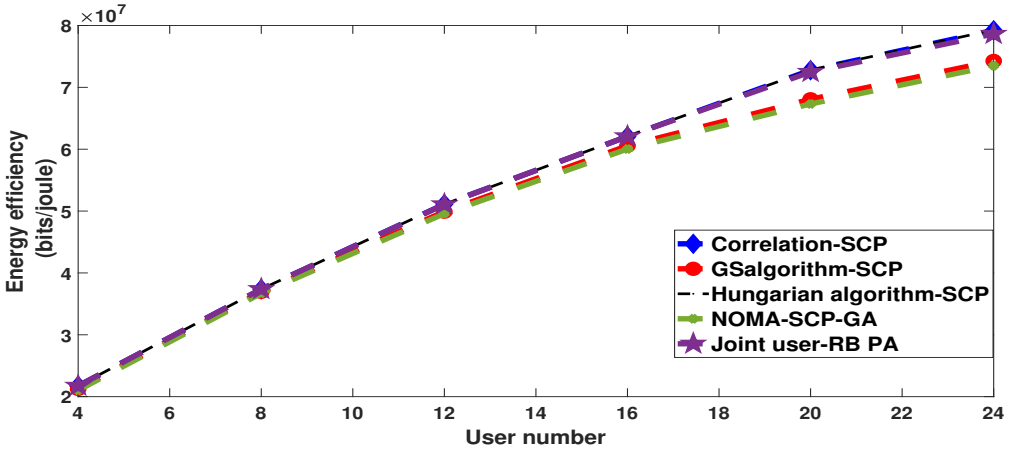

Figure 3. EE versus number of users, with $A = 36$ BS antennas, ZF beamforming.

Figure 4 demonstrates the effect of the increase in the number of BS antennas on EE calculations for different algorithms with $U = 10$ users. The overall performance shows that the increase in A leads to an increase in EE for low A values till reaching a value of $A = 20$. Then, the performance changes. EE decreases with increasing A because the increase in power consumed in a large number of antennas reduces EE, even with the increase in rate.

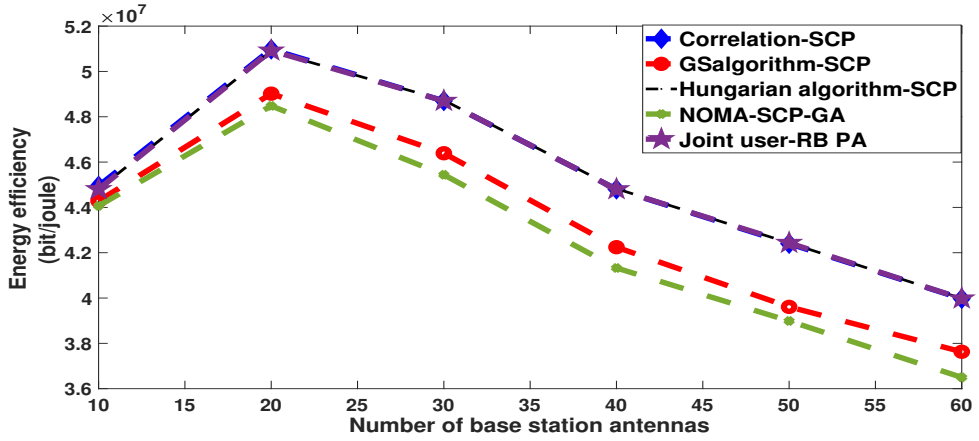

Figure 4. EE versus number of BS antennas, with $U = 10$ users, ZF beamforming.

Figure 5 demonstrates the effect of the increase in the number of BS antennas on SE calculations for different algorithms with $U = 10$ users. The overall performance in the results shows that the increase in A leads to an increase in spectral efficiency. Correlation-SCP, Hungarian algorithm-SCP, and joint user-RB PA have the best performance. NOMA-SCP-GA has the worst performance which means that NOMA groups formed by the greedy algorithm and their allocated power led to the lowest SE results.

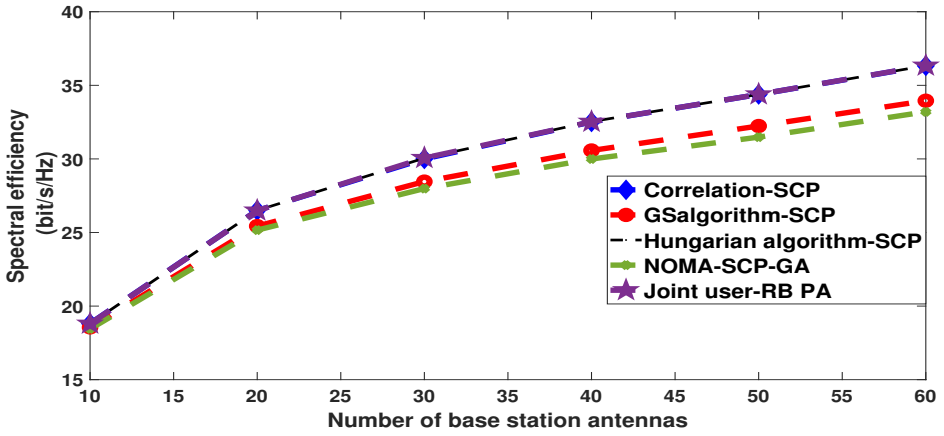

Figure 5. The spectral efficiency versus number of BS antennas, with $U = 10$ users, ZF beamforming.

Figure 6 depicts the power consumed in user pairing algorithms. It shows the high power consumption provided by the correlation-based pairing method as a result of the high computational complexity followed by the swap algorithm used for pairing in (joint user-RB PA) due to the swap process. The GS algorithm and GA algorithm in (NOMA-SCP-GA) achieve the lowest power consumption due to their low computational complexity.

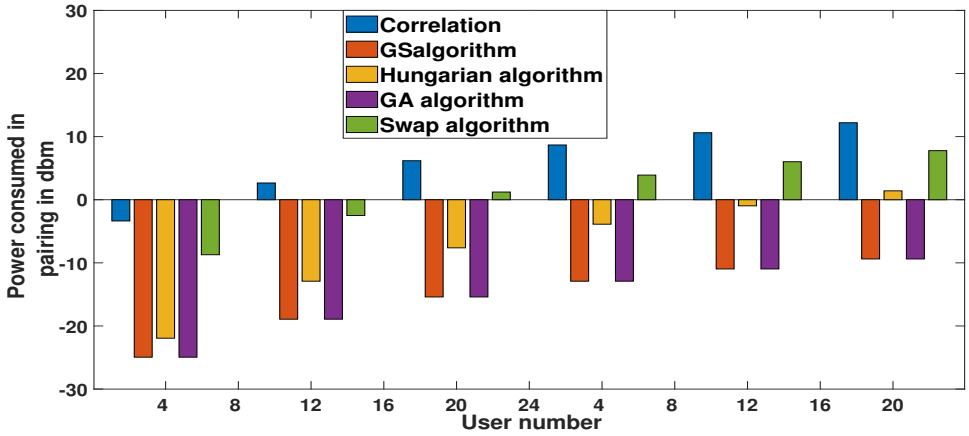

Figure 6. Power consumed in user paring in dBm versus user number, with $A = 36$ BS antennas.

The complexity is calculated in Table 5 for the pairing approaches used in our work. Complexity is computed for $A = 36$ BS antennas and $U = 20$ users. According to formulas in the complexity analysis section, correlation-based pairing has the highest complexity followed by the Hungarian algorithm, then the GS algorithm.

Table 5. Complexity calculations for different pairing approaches.

Pairing Approach	Complexity
GS algorithm	100
Hungarian algorithm	1000
Correlation	14,400

Figure 7 shows the effect of increasing the number of BS antennas on complexity. The complexity of correlation-based pairing increases linearly with A while the complexities of the Hungarian algorithm and GS algorithm are constant with respect to A.

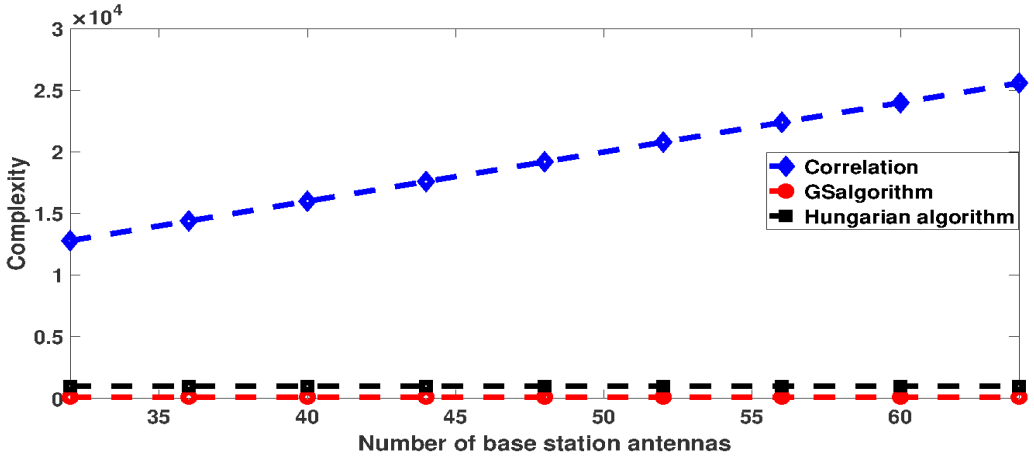

Figure 7. Complexity versus number of BS antennas, with U = 20 users.

Figure 8 demonstrates the relation between the number of users and the complexity at a specific number of BS antennas. The complexity of the three approaches is increasing with the increase in the number of users. The highest complexity is for the correlation based pairing, while the lowest is for the GS algorithm.

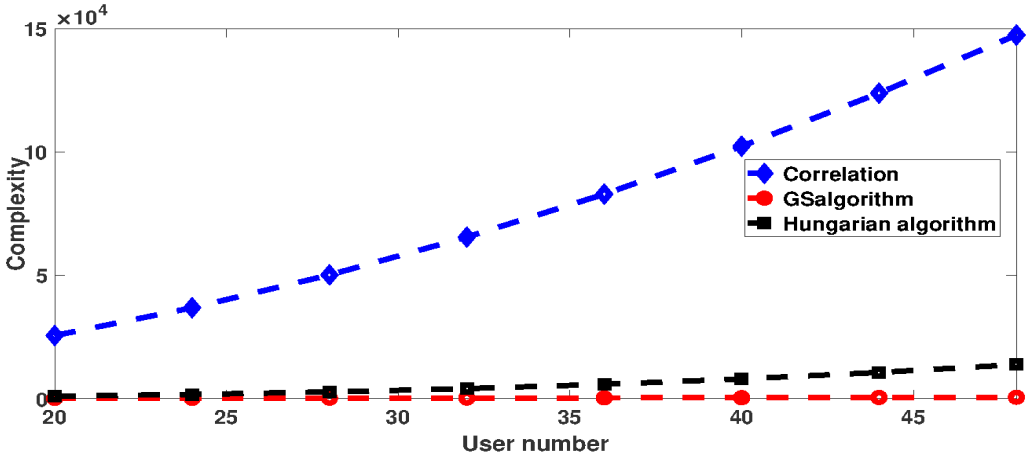

Figure 8. Complexity versus User number, with A = 64 BS antennas.

8. Conclusions

In this paper, the EE optimization problem for the downlink NOMA-based massive MIMO system is investigated with the constraints of BS power transmission and minimum user rate. The problem is decoupled into the user pairing subproblem and fair power allocation subproblem to reduce complexity. For the user pairing subproblem, three different pairing methods were employed for pairing cell-center users with cell-edge users to

guarantee maximum EE for NOMA groups. For the power allocation subproblem, we mathematically formulated the max-min EE into a non-convex fractional programming problem, which is transformed into a sequence of subtractive form, followed by the SCP approach to obtain the optimal solution. A practical detailed power consumption model is introduced for the downlink NOMA-based scheme. Simulation results show that the NOMA-based scheme outperforms the mMIMO-based scheme for the large number of users. Moreover, the increase in the number of BS antennas reduces the EE of NOMA-based scheme due to increased power consumption. Additionally, the correlation pairing method has the highest computational complexity compared to the other two pairing methods. The correlation-SCP and Hungarian algorithm-SCP achieve identical EE results and outperform the GS algorithm-SCP. The Hungarian algorithm-SCP gives the same superior performance of the joint user-RB PA method but with lower computational complexity and outperforms the NOMA-SCP-GA method. In the future, our work will investigate the design of a beamforming technique for the NOMA-based scheme that improves the performance of NOMA groups and makes the results of different pairing algorithms more distinctive.

Author Contributions: Conceptualization, M.A.E.-g.; Investigation, M.A.E.-g.; Methodology, F.N.; Software, M.A.E.-g.; Supervision, F.N.; Validation, M.R.E.-m.; Visualization, M.M.I.; Writing—original draft, M.A.E.-g.; Writing—review & editing, M.R.E.-m. All authors have read and agreed to the published version of the manuscript.

Funding: This research received no external funding.

Data Availability Statement: Not applicable.

Conflicts of Interest: The authors declare no conflict of interest.

Abbreviations

List of Acronyms

EE	Energy Efficiency
NOMA	Non-Orthogonal Multiple Access
SCMA	Sparse Code Multiple Access
PDMA	Pattern Division Multiple Access
MIMO	Multiple Input Multiple Output
NLoS	Non-Line of Sight
SIC	Successive Interference Cancellation
SCP	Sequential Convex Programming
SE	Spectral Efficiency
IOT	Internet of Things
CSI	Channel State Information
5G	Fifth Generation of Cellular Communications
BS	Base Station
MS	Mobile Station
D2D	Device-to-Device
KKT	Karush–Kuhn–Tucker
MCMC-NOMA	Multi-Cell Multi-Carrier Non-Orthogonal Multiple Access
GRASP	Greedy Randomized Adaptive Search
SSD	Stochastic Sample Greedy
DPCA	Dynamic Power and Channel Allocation
WAR	Weighted Achievable Rate
AmBC	Ambient Backscatter Communication
FTPC	Fractional Transmitting Power Control
DC	Difference of Convex
SCA	Successive Convex Approximation
SDMA	Spatial Division Multiple Access
JT-CoMP	Joint Transmission Coordinated Multi-Point

List of Symbols

DPS-CoMP	Dynamic Point Selection Coordinated Multi-Point
QoS	Quality of Service
ZF	Zero Forcing
TDD	Time Division Duplex
U	Number of users
A	Number of base station antennas
u_c	Cell-center user
U_c	Number of cell-center users
u_e	Cell-edge user
U_e	Number of cell-edge users
$\mathbf{g}_u$	Downlink channel vector of user u
β_u	Large-scale fading coefficient
$\mathbf{h}_u$	Channel response of user u
$\mathbf{I}_A$	Identity matrix
R	Throughput
γ	Power consumption
$ETpower$	Effective transmitted power
$Cpower$	Circuit power consumption
ξ	Efficiency of power amplifier
q_u	BS transmitted power to user u
$P_{cod/dec}$	Power consumed by encoding, decoding
P_{bh}	Power consumed by signaling of backhaul
P_{sp}	Power consumed by digital signal processing
P_{fix}	Load independent power of infrastructure and power of control signaling
P_{tc}	Power consumed by transceiver chains
P_{BS}	Power required to operate the circuit components of BS
P_{lo}	Power consumed by local oscillator
P_{UE}	Power consumed by circuit components in user equipment
P_{cod}	Power required to encode throughput at base station
P_{dec}	Power required to decode throughput at the user equipment
P_{bh}	Power required by load dependent backhaul
P_{bt}	Power of backhaul traffic
P_{ce}	Power consumed in channel estimation
B	Communication bandwidth
M	Number of samples per coherence block
L_{bs}	Computational efficiency of BS
P_{sp}	Power consumed by digital signal processing
P_{sp-t}	Power consumed in downlink transmission
P_{sp-c}^{DL}	Power required for computing beamforming vector
τ_d	Downlink data in each coherence interval
δ_{cost}	Cost matrix
$\hat{\boldsymbol{h}}$	Estimated channel response
ρ_{u_c,u_e}	Correlation between the channel of cell-center user u_c and cell-edge user u_e
R_{min}	Minimum data rate for cell-center user
$\mathbf{w}_u$	ZF beamforming vector for user u
$\eth$	Smooth optimization function

References

1. Ding, Z.; Lei, X.; Karagiannidis, G.K.; Schober, R.; Yuan, J.; Bhargava, V. A survey on non-orthogonal multiple access for 5G networks: Research challenges and future trends. *arXiv* **2017**, arXiv:1706.05347.
2. Marques da Silva, M.; Dinis, R. Power-Ordered NOMA with Massive MIMO for 5G Systems. *Appl. Sci.* **2021**, *11*, 3541. [CrossRef]
3. Marques da Silva, M.; Dinis, R.; Martins, G. On the Performance of LDPC-Coded Massive MIMO Schemes with Power-Ordered NOMA Techniques. *Appl. Sci.* **2021**, *11*, 8684. [CrossRef]
4. Nguyen, H.V.; Kim, H.M.; Kang, G.M.; Nguyen, K.H.; Bui, V.P.; Shin, O.S. A Survey on Non-Orthogonal Multiple Access: From the Perspective of Spectral Efficiency and Energy Efficiency. *Energies* **2020**, *13*, 4106. [CrossRef]
5. Ding, Z.; Liu, Y.; Choi, J.; Sun, Q.; Elkashlan, M.; Chih-Lin, I.; Poor, H.V. Application of non-orthogonal multiple access in LTE and 5G networks. *IEEE Commun. Mag.* **2017**, *55*, 185–191. [CrossRef]

6. Islam, S.; Avazov, N.; Dobre, O.; Kwak, K. Power-domain non-orthogonal multiple access (NOMA) in 5G systems: Potentials and challenges. *IEEE Commun. Surv. Tutor.* **2017**, *19*, 712–742. [CrossRef]
7. Dai, L.; Wang, B.; Ding, Z.; Wang, Z.; Chen, S.; Hanzo, L. A survey of non-orthogonal multiple access for 5G. *IEEE Commun. Surv. Tutor.* **2018**, *20*, 2294–2323 . [CrossRef]
8. Zhang, Z.; Sun, H.; Qingyang, R. Downlink and uplink non-orthogonal multiple access in a dense wireless network. *IEEE J. Sel. Areas Commun.* **2017**, *35*, 2771–2784. [CrossRef]
9. Yang, Z.; Pan, C.; Xu, W.; Pan, Y.; Chen, M.; Elkashlan, M. Power control for multi-cell networks with non-orthogonal multiple access. *IEEE Trans. Wirel. Commun.* **2018**, *17*, 927–942. [CrossRef]
10. Choi, J. Minimum power multicast beamforming with superposition coding for multiresolution broadcast and application to NOMA systems. *IEEE Trans. Commun.* **2015**, *63*, 791–800. [CrossRef]
11. Ding, Z.; Fan, P.; Poor, H.V. Impact of user pairing on 5G nonorthogonal multiple-access downlink transmission. *IEEE Trans. Vehic. Tech.* **2016**, *65*, 6010–6023. [CrossRef]
12. Yuan, W.; Wu, N.; Zhang, A.; Huang, X.; Li, Y.; Hanzo, L. Iterative Receiver Design for FTN Signaling Aided Sparse Code Multiple Access. *IEEE Trans. Wirel. Commun.* **2020**, *19*, 915–928. [CrossRef]
13. Dai, X.; Zhang, Z.; Bai, B.; Chen, S.; Sun, S. Pattern Division Multiple Access: A New Multiple Access Technology for 5G. *IEEE Wirel. Commun.* **2018**, *25*, 54–60. [CrossRef]
14. Jungnickel, V.; Manolakis, K.; Zirwas, W.; Panzner, B.; Braun, V.; Lossow, M.; Sternad, M.; Apelfrojd, R.; Svensson, T. The role of small cells, coordinated multipoint, and massive MIMO in 5G. *IEEE Commun. Mag.* **2014**, *52*, 44–51. [CrossRef]
15. Alimi, I.A.; Patel, R.K.; Muga, N.J.; Pinto, A.N.; Teixeira, A.L.; Monteiro, P.P. Towards Enhanced Mobile Broadband Communications: A Tutorial on Enabling Technologies, Design Considerations, and Prospects of 5G and beyond Fixed Wireless Access Networks. *Appl. Sci.* **2021**, *11*, 10427. [CrossRef]
16. Gkonis, P.K.; Trakadas, P.T.; Kaklamani, D.I. A Comprehensive Study on Simulation Techniques for 5G Networks: State of the Art Results, Analysis, and Future Challenges. *Electronics* **2020**, *9*, 468. [CrossRef]
17. Gao, Y.; Vinck, H.; Kaiser, T. Massive MIMO antenna selection: Switching architectures, capacity bounds and optimal antenna selection algorithms. *IEEE Trans. Signal Process.* **2018**, *66*, 1346–1360. [CrossRef]
18. Gao, X.; Edfors, O.; Tufvesson, F.; Larsson, E. Massive MIMO in real propagation environments: Do all antennas contribute equally? *IEEE Trans. Commun.* **2015**, *63*, 3917–3928. [CrossRef]
19. Björnson, E.; Hoydis, J.; Sanguinetti, L. Massive MIMO Networks: Spectral, Energy, and Hardware Efficiency. *Found. Trends Signal Process.* **2017**, *11*, 154–655. [CrossRef]
20. Wang, J.; Song, X.; Ma, Y. A Novel Resource Allocation Scheme in NOMA-Based Cellular Network with D2D Communications. *Future Internet* **2020**, *12*, 8. [CrossRef]
21. Senel, K.; Cheng, H.V.; Björnson, E.; Larsson, E.G. What Role Can NOMA Play in Massive MIMO? *IEEE J. Sel. Top. Signal Process.* **2019**, *13*, 597–611. [CrossRef]
22. Ali, Z.J.; Noordin, N.K.; Sali, A.; Hashim, F.; Balfaqih, M. Novel Resource Allocation Techniques for Downlink Non-Orthogonal Multiple Access Systems. *Appl. Sci.* **2020**, *10*, 5892. [CrossRef]
23. Adam, A.; Wan, X.; Wang, Z. Energy Efficiency Maximization for Multi-Cell Multi-Carrier NOMA Networks. *Sensors* **2020**, *20*, 6642. [CrossRef] [PubMed]
24. Nguyen, K.H.; Nguyen, H.V.; Le M.T.; Cao, T.X.; Shin, O.S. Rate Fairness and Power Consumption Optimization for NOMA-Assisted Downlink Networks. *Energies* **2021**, *14*, 58. [CrossRef]
25. Chen, R.; Shu, F.; Lei, K.; Wang, J.; Zhang, L. User Clustering and Power Allocation for Energy Efficiency Maximization in Downlink Non-Orthogonal Multiple Access Systems. *Appl. Sci.* **2021**, *11*, 716. [CrossRef]
26. Xu, Z.; Petrunin, I.; Li, T.; Tsourdos, A. Efficient Allocation for Downlink Multi-Channel NOMA Systems Considering Complex Constraints. *Sensors* **2021**, *21*, 1833. [CrossRef]
27. Li, H.; Li, H.; Zhou, Y. Optimization Algorithms for Joint Power and Sub-Channel Allocation for NOMA-Based Maritime Communications. *Entropy* **2021**, *23*, 1454. [CrossRef]
28. Liu, Q.; Sun, S.; Hou, J.; Jia, H.; Kadoch, M. Resource Allocation in NOMA-Assisted Ambient Backscatter Communication System. *Electronics* **2021**, *10*, 3061. [CrossRef]
29. Wang, J.; Wang, Y.; Yu, J. Joint Beam-Forming, User Clustering and Power Allocation for MIMO-NOMA Systems. *Sensors* **2022**, *22*, 1129. [CrossRef]
30. Maeng, J.; Dahouda, M.K.; Joe, I. Optimal Power Allocation with Sectored Cells for Sum-Throughput Maximization in Wireless-Powered Communication Networks Based on Hybrid SDMA/NOMA. *Electronics* **2022**, *11*, 844. [CrossRef]
31. Abuajwa, O.; Roslee, M.; Yusoff, Z.B.; Chuan, L.L.; Leong, P.W. Resource Allocation for Throughput versus Fairness Trade-Offs under User Data Rate Fairness in NOMA Systems in 5G Networks. *Appl. Sci.* **2022**, *12*, 3226. [CrossRef]
32. Wu, J.; Sun, L.; Jia, Y. User Pairing and Power Allocation for NOMA-CoMP Based on Rate Prediction. *Information* **2022**, *13*, 200. [CrossRef]
33. Fang, F.; Zhang, H.; Cheng, J.; Leung, V.C.M. Energy efficient resource allocation for downlink non-orthogonal multiple access network. *IEEE Trans. Commun.* **2016**, *64*, 3722–3732. [CrossRef]
34. Zamani, M.R.; Eslami, M.; Khorramizadeh, M.; Ding, Z. Energy efficient power allocation for NOMA with imperfect CSI. *IEEE Trans. Veh. Technol.* **2019**, *68*, 1009–1013. [CrossRef]

35. Liu, G.; Wang, R.; Zhang, H.; Kang, W.; Tsiftsis, T.A.; Leung, V.C.M. Super-modular game-based user scheduling and power allocation for energy-efficient NOMA network. *IEEE Trans. Wirel. Commun.* **2018**, *17*, 3877–3888. [CrossRef]
36. Ali, Z.J.; Noordin, N.K.; Sali, A.; Hashim, F.; Balfaqih, M. An efficient method for resource allocation and user pairing in downlink non-orthogonal multiple access system. In Proceedings of the 2019 IEEE 14th Malaysia International Conference on Communication (MICC), Selangor, Malaysia, 2–4 December 2019; pp. 124–129.
37. Marcano, A.S.; Christiansen, H.L. Impact of NOMA on Network Capacity Dimensioning for 5G HetNets. *IEEE Access* **2018**, *6*, 13587–13603. [CrossRef]
38. Zeng, M.; Hao, W.; Dobre, O.A.; Poor, H.V. Energy-Efficient Power Allocation in Uplink mmWave Massive MIMO with NOMA. *IEEE Trans. Vehic. Tech.* **2019**, *68*, 3000–3004. [CrossRef]
39. Zeng, M.; Yadav, A.; Dobre, O.A.; Poor, H.V. Energy-Efficient Joint User-RB Association and Power Allocation for Uplink Hybrid NOMA-OMA. *IEEE Internet Things J.* **2019**, *6*, 5119–5131. [CrossRef]
40. Rashid, B.; Ahmad, A.; Saleem, S.; Khan, A. Joint energy efficient power and subchannel allocation for uplink MC-NOMA networks. *Int. J. Commun. Syst.* **2020**, *33*, e4606. [CrossRef]
41. Islam, S.R.; Zeng, M.; Dobre, O.A.; Kwak, K.S. Resource Allocation for Downlink NOMA Systems: Key Techniques and Open Issues. *IEEE Wirel. Commun.* **2018**, *25*, 40–47. [CrossRef]
42. Ali, Z.J.; Noordin, N.K.; Sali, A.; Hashim, F. Fair Energy-Efficient Resource Allocation for Downlink NOMA Heterogeneous Networks. *IEEE Access* **2020**, *8*, 200129–200145. [CrossRef]